Lisa Michelle Dahl
June 04, 2008
CHEM E 499 - Finlayson

Mixing Properties of an Optimized SAR Mixer (2D and 3D Models)

I. Introduction

While mixing is the most common unit-operation in chemical industrial processes, optimizing mixing in microchemical processes requires further investigation in various geometries. One method of microchemical mixing includes the Split-and-Recombine (SAR) approach, which encourages uniform mixing through the mechanical formation of vertical, alternating layers of two concentrations. The process, illustrated in Figure 1, is known as fine homogenous multi-lamination and is useful for accomplishing a certain degree of mixing under moderate pressure drops (3, 65).

Figure 1: The four steps to one "step" of the SAR approach is depicted above. An inlet feed of two adjacent concentrations enters in step one. The flow is split horizontally in step two. In step three, the two split streams are rejoined side by side. The width of the stream is then decreased to reshape the layers to the minimum channel cross section. The layers formed in step four are known as homogenous lamellae. Source: Schönfeld, F. et al. "An optimized split-and-recombine micro-mixer with uniform 'chaotic' mixing." *Lab Chip*, 2004, **4**, 65-69.

The current micro-mixer of choice, the caterpillar mixer, effective mixing is achieved in flow with high Reynolds numbers (Re); however, for laminar flow (characterized by a low Reynolds number) the layers formed are subject to internal friction and the lamellae become non-uniform (3, 66). Schönfeld et al introduces an optimized SAR mixer, illustrated in Figure 2, which is mechanically designed to separate the layers as depicted in Figure 1.
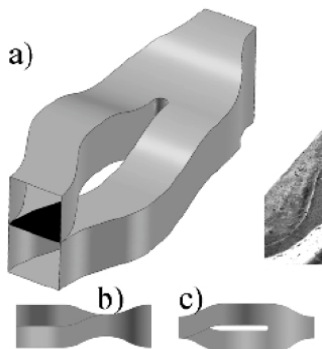

Figure 2: The optimized SAR mixer as introduced by Schönfeld et al. The overall geometry in 3D is shown in (a), whereas the side and top views are shown in (b) and (c) respectively. Source: Schönfeld, F. et al. "An optimized split-and-recombine micro-mixer with uniform 'chaotic' mixing." *Lab Chip*, 2004, **4**, 65-69

Its differences over a caterpillar mixer include the more dramatic horizontal separation of the inlet flow, the split sub-streams are allowed to travel for a longer length, and the reshaping

geometry to minimize internal friction. Its operation is split into three steps: splitting, rearranging and recombination, and reshaping (3, 67). In addition, this geometry can be repeated in series such that a "step" is defined as the flow running through a single link in the "chain." The goal of homogenous vertical lamellae is then achieved.

II. Approach and Model

The primary goal is to achieve the best mixing possible within the geometry; the subsidiary goal is to characterize it. Mixing characterization is typically quantitatively measured through models to allow for comparison and optimization. A common characteristic for chemical engineering applications is known as the "mixing cup" concentration, $c_{mixing\,cup}$ (2, 198). This involves the overall concentration and velocity profile to measure the mass flux over a given cross-sectional area within the geometry, as defined in equation A.

$$c_{mixingcup} = \frac{\int_A c(x,y,z) \cdot v(x,y)dxdy}{\int_A v(x,y)dxdy} = \frac{\int_A c \cdot vdA}{\int_A vdA} \qquad [A]$$

The variance of the mixing cup concentration is then defined in equation B.

$$\sigma_{mixingcup} = \frac{\int_A [c(x,y,z) - c_{mixingcup}]^2 \cdot v(x,y)dxdy}{\int_A v(x,y)dxdy} = \frac{\int_A [c - c_{mix}]^2 \cdot vdA}{\int_A vdA} \qquad [B]$$

When the average velocity over the geometry is defined as 1, the v terms can be neglected to find the optical mixing cup concentration value.

SAR mixers are also associated with their own set of mixing characteristics. Its performance is typically described by its interfacial stretching due to chaotic advection within th flow (3, 65). For our current interests, SAR mixing is also known to exhibit a linear pressure drop over the geometry repeated in series as seen in equation C (3, 66).

$$\Delta p = n \cdot p_0 \qquad [C]$$

The pressure drop for fully developed flow over pipe geometry is typically measured using the Hagen-Pouiseuille law with an added excess pressure value specific to the geometry. As there is no current excess pressure coefficient for this geometry, the pressure drop will be measured using the model in COMSOL Multiphysics.

A two-dimensional model of the optimized SAR mixer was created using COMSOL Multiphysics version 3.4. The modules Steady-State Navier-Stokes and Convection and

Diffusion under the Chemical Engineering Module folder were used. Schönfeld et al models the geometry with a minimum channel cross section of 1mm and an overall length of 6mm. These values motivated the nondimensional standard choices, where standard length x_s is 200 _m, the average velocity v_s is 0.005 m/s and the pressure standard p_s is 0.005 Pa. The density _ of the subdomain was set to 1000 kg/m^3 and the viscosity _ was set to 10^{-3} Pa·s. The overall length of the non-dimensional geometry is 6 with an additional entrance of length 1 for the entering flow of split concentration (totaling a length of 7). The Reynolds number, based on the standard values, is equivalent to 1 for very laminar flow. The model as screen-capped in COMSOL is shown in Figure 3.
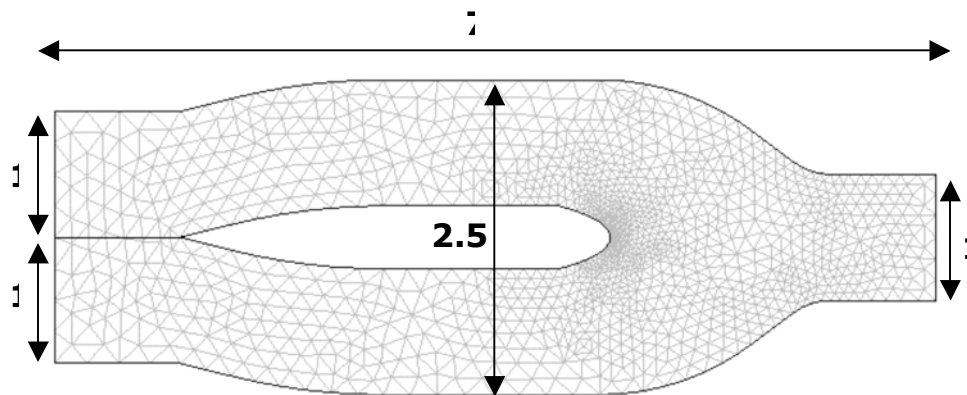

Figure 3: The two-dimensional model of the optimized SAR mixer as modeled in COMSOL Multiphyics 3.4, rotated by 90° counter clockwise. The minimum channel width is standardized to 1. From this view, the inlets are at the left-side and flow goes from left to right. The second level mesh is shown (Fine) with 2616 elements and 17579 degrees of freedom.

For the Navier-Stokes module, all walls were set to a No-Slip boundary condition while the inlet has laminar flow with an average velocity of 1. The outlet has a defined pressure of 0 Pa with no viscous stress. Under the Convection and Diffusion module, the subdomain has a dimensionless diffusivity D defined as 1/Pe, where Pe is the Peclet number and varies from 100 to 1000. A step concentration profile of 1 over half the inlet length to 0 for the other half is defined, where the left-hand inlet (between x = -1 and 0) is defined as (x<=-0.5)*1+(0.5>x)*0 and the right-hand inlet (between x = 0 and 1) is (0<x<0.5)*1+(0.5<=x<=1)*0. Convective flux is set for the outlet. All of the walls are given an Insulation/Symmetry boundary condition.

As the actual geometry of the optimized SAR mixer has overlaps and depth, some changes are necessary to depict the geometry in two dimensions. It is necessary to model the split at the beginning of the geometry, thus two inlets with the same entering velocity and

concentration profile are set. While the depth changes in the substream section may have some effect on the mixing within the geometry, only the side-to-side bends can be modeled in the two-dimensional geometry. While the top view in Figure 2 shows the substreams are physically split by only about 1/4 the minimum channel width, in order to depict the angle at which the streams bend away from the inlet a physical separation of _ the minimum channel width, or 0.5 in the model, is used. This changes the angle at which the streams are recombined near the end of the model. As these compromises in the geometry may affect the mixing results and deviate from actual mixing seen in three dimensions, the two-dimensional model must be taken as only an approximation.

A three-dimensional model of the SAR mixer was also examined in COMSOL. Unfortunately, it was also necessary to approximate the geometry with general features due to the limitations of efficient modeling in COMSOL. If the geometry were able to converge without open holes or faces, the 3D model is expected to look like Figure 8.
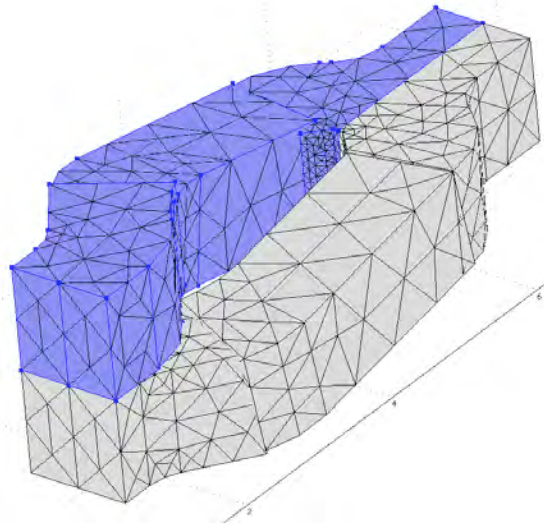

Figure 8: The expected 3D model in COMSOL is shown above using approximations with shapes. The two inlets are shown to the bottom left, where the stacked inlets (the split) is an important feature of the SAR mixer. The left side is highlighted in purple to show the separation between the two split streams and the top right represents the outlet, where both streams combine to a single channel.

Instead of the model depicted in Figure 8, an extrusion of the two-dimensional model was performed. This forces the inlets to be modeled from side by side instead of the more accurate stacked version shown in Figure 8. In addition, the z-directional depth of the device is not modeled and the center of both inlets and the outlet lie on the same plane, where in the more accurate model the center of each inlet is 0.5 standard dimensions away from the outlet's center

plane. The top and bottom walls of the device are both under no-slip boundary conditions. The model used for three-dimensional representation is shown in Figure 9.
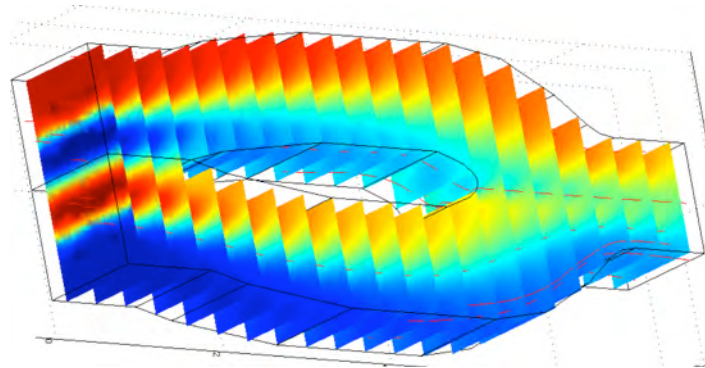

Figure 9: The 3D model used for concentration characterization is depicted, where the two inlets are to the left and the flow goes towards the right. The equivalent boundary conditions and subdomain settings are used for the walls, the inlets and the outlets of the geometry. The solution is shown for a Peclet number of 1000 and using the third mesh (30081 elements, 201852 degrees of freedom).

Both the two-dimensional and three-dimensional geometries, including the two-dimensional geometries in series, were examined for their mixing cup and optical concentration values and resulting variances using the boundary integration tool across the outlets in COMSOL Multiphysics 3.4.

III. Results

First, the two-dimensional geometry was solved under the Navier-Stokes and Convection/Diffusion models to ensure that the flow was fully developed and that the expected homogenous lamellae layers are achieved. This is confirmed by looking at the streamlines and surface plot of the concentration, as screen-captured in Figure 4.
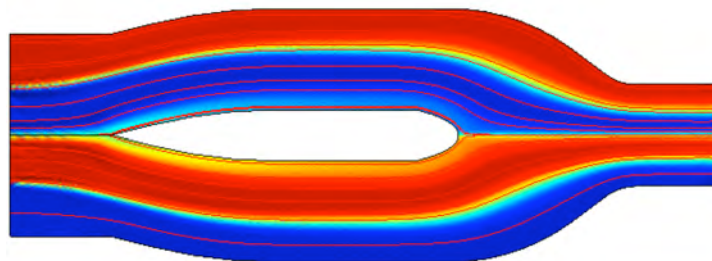

Figure 4: The solution to the two-dimensional model with the velocity streamlines and concentration surface plot is depicted above, rotated by 90° counter clockwise. The red represents a concentration of 1 whereas indigo is a concentration of 0, equal mixing is green with a value of 0.5, and the variation in color represents the concentration gradient. For a Peclet number of 1000 on Mesh #3 (10464 elements and 69615 degrees of freedom), the lamellae layers are clearly shown.

5

The mixing characteristics for Pe = 1000 over three meshes of increasing complexity, where the mixing cup concentration values are based on the outlet values, are displayed in Table 1.

Table 1: Mixing Characteristics for the 2D Model of an Optimized SAR Mixer, Pe = 1000

Mesh #	1	2	3
# of Elements	654	2616	10464
Degrees of Freedom	4539	17579	69615
C_{mix} with v, (mol/m^3)	0.505	0.504	0.500
C_{var} with v, (mol^2/m^6)	0.060	0.126	0.128
$C_{optical}$ no v, (mol/m^2)	0.506	0.504	0.500
C_{optvar} no v, (mol^2/m^5)	0.119	0.148	0.147
_P (Pa)	0.430	0.427	0.427

The raw results and data used for calculation each of the results can be viewed in the appendix. Over increasing mesh parameters the concentration characteristics are seen to converge, such that Mesh #3 can be considered the characteristic results for a Peclet number of 1000.

Though an optimal mixing cup concentration of 0.50 is achieved through just one geometry run, the mixing cup concentration variance was also examine for the geometry in series. An example of modeling the geometry in a series of 2 is depicted in Figure 5.
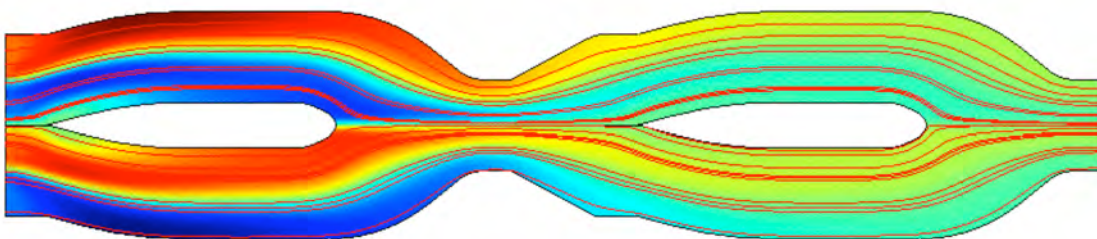

Figure 5: The solution for the two-dimensional model in a series of 2 is shown, rotated by 90° counter clockwise, for a Peclet number 1000 and on the third mesh (5236 elements, 35144 degrees of freedom).

The variance of the mixing cup concentration effects over the optimized SAR mixer in series is depicted in Figure 6 on a natural logarithmic scale.

Mixing Cup Concentration Characteristic Effect of the SAR Mixer in Series
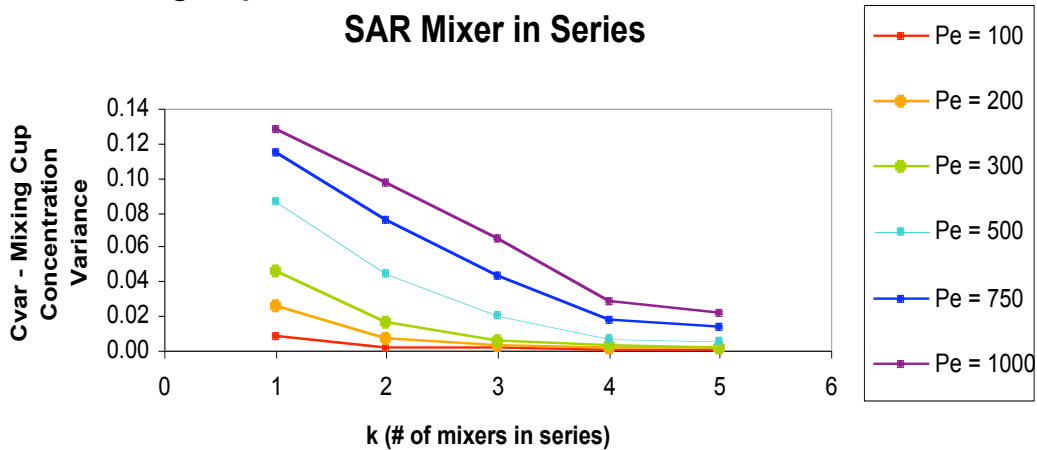

Figure 6: The change in the mixing cup concentration variance, over the number of mixers in series, is depicted above for six different Peclet number values to show six different values of flow.

From Figure 6, we see that with increasing Peclet number the mixing cup concentration variance within the outlet decreases, as expected for higher diffusion constants. Over the increase in series or steps of the geometry (k), Figure 6 shows a gradual decrease in the variation. For a Peclet number of 1000, the variance changes from 0.128 for one step to 0.021 for five steps. This range is made even smaller for decreasing Peclet numbers. This confirms the improved uniform mixing as more steps of the geometry are added. Raw data values for Figure 6 can be viewed in the appendix.

Figure 7 similarly demonstrates the trend for the optical concentration variance over a series of one to five steps.

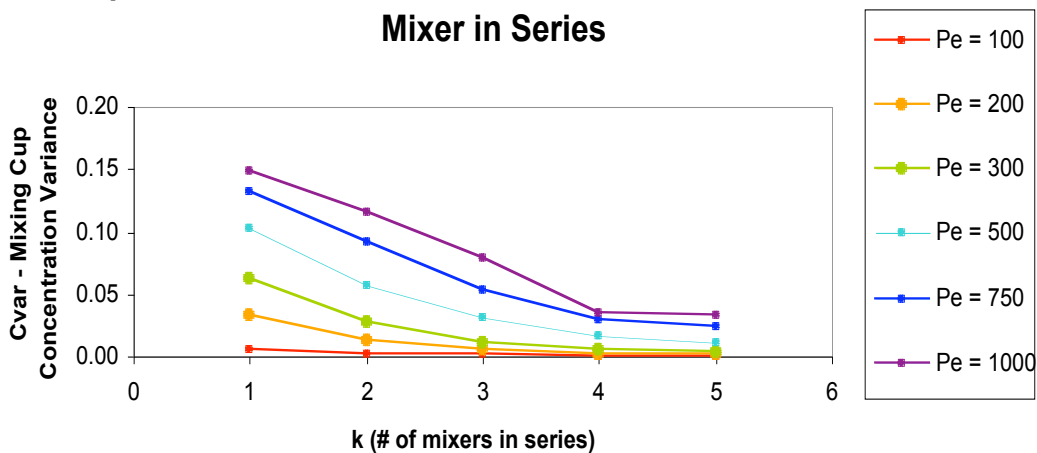## Optical Concentration Characteristic Effect of the SAR Mixer in Series

Figure 7: The change in the optical concentration variance, over the number of mixers in series, is depicted above for six different Peclet number values to show six different values of flow.

Figure 7 demonstrates a similar trend to Figure 6, where the optical concentration variance decreases both for increasing Peclet number and increasing number of steps, k. This shows that for either mixing cup or optical applications, more uniform mixing can be achieved with larger Peclet numbers and with the geometry in series.

Figure 8 compares the difference between the mixing cup and optical concentration variances for the optical SAR mixer in only one step (not in a series).
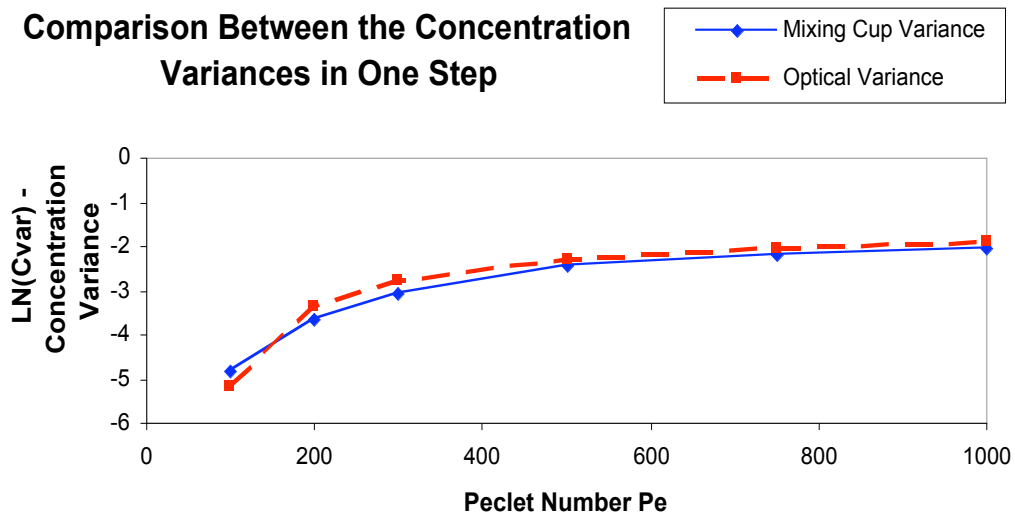

Figure 8: The change in the natural log of the mixing cup and optical concentration variances is plotted over varying Peclet numbers from 100 to 1000, representing changes in diffusivity.

Based on Figure 8, there is a slight deviation between the two values but due to the values of these differences (0.02 at its highest, for a Peclet number of 1000) the relative variances can be considered equivalent.

The mixing cup and optical concentration values for the three-dimensional model are evaluated in a method similar to the two-dimensional parameters, where the characteristics are evaluated at the inlet and the pressure drop is evaluated at the inlets and averaged (assuming the outlet has a pressure drop of 0 with viscous stresses). The results for the three-dimensional model can be viewed in Table 2.

Table 2: Mixing Characteristics for the 3D Model of an Optimized SAR Mixer, Pe = 1000

Mesh #	1	2	3
# of Elements	2360	9270	30081

8

Degrees of Freedom	34900	76495	201852
C_{mix} with v, (mol/m^3)	0.522	0.509	0.493
C_{var} with v, (mol^2/m^6)	0.080	0.106	0.126
$C_{optical}$ no v, (mol/m^2)	0.505	0.514	0.507
C_{optvar} no v, (mol^2/m^5)	0.167	0.141	0.147
_P (Pa)	0.881	0.881	0.881

The mesh refinement is similar to the 2-D case where the characteristic values approach the values shown in the third mesh, which was the finest mesh with a solution. The mixing cup and optical concentration values are both very close to 0.5, demonstrating efficient mixing. In addition, the variances are lower than the values obtained for the two-dimensional case. A comparison between these characteristics can be seen in Table 3.

Table 3: Mixing Characteristic Differences between 2D and 3D models, Pe = 1000

Model	2D	3D	_
C_{mix}, (mol/m^3)	0.5	0.493	*0.007*
C_{var}, (mol^2/m^6)	0.128	0.126	*0.002*
$C_{optical}$, (mol/m^2)	0.5	0.507	*0.007*
$C_{opt,var}$, (mol^2/m^5)	0.147	0.147	*0*
_P (Pa)	0.427	0.881	*0.454*

The small difference between the mixing cup concentration and optical concentration values between the two-dimensional and three-dimensional models suggests that the simplified two-dimensional model suffices for examining the mixing within the geometry. The differences between the two-dimensional and three-dimensional variances are also comparatively small, suggesting further equivalence between the two models.

IV. Suggestions for Improved Mixing

Based on the results, particularly demonstrated in Figure 6, mixing is improved by increasing the number of the optimal SAR mixer geometry in series. However, a uniform mixing cup concentration of 0.5 is achieved in just one step of the SAR mixer. The variance

decreases with decreasing Peclet number, showing that more uniform mixing is achieved with lower Peclet numbers whereas the lamellae are achieved for high Peclet numbers up to 1000.

To improve the mixing for the SAR mixer geometry in a single step, increasing the length the middle section of the geometry with the split streams is suggested. This allows for the split streams to internally mix further before being recombined to form the lamellae layers. As more defined lamellae layers lead to a higher mixing cup concentration variance, allowing for further mixing will decrease the variance in the final mixing cup concentration value. In addition, using as many of the geometry in series as possible will improve uniform mixing as soon as by the second step, as shown in Figure 5. If the formation of the homogenous lamellae layers is the goal, however, then it is suggested to use as few of the geometry in series and to shorten the entrance and recombination sections to minimize the amount of internal mixing between the splitting sections.

V. Literature Comparison

The optimized Split-and-Recombine (SAR) mixer is presented in the literature "An optimized split-and-recombine micro-mixer with uniform 'chaotic' mixing" by Schönfeld, F. et al. The geometry is designed to achieve uniform mixing through the continuous splitting and reformation of homogenous lamellae layers in a flow with a binary step concentration profile. Schönfeld et al investigates the mixing characteristics of this geometry through theoretical analysis and visual verification of layer formation. Our investigation has involved mixing cup and optical concentration measurements and the concentration variance for these two characterizations. The results achieved through modeling in COMSOL confirm the results presented in the literature despite the different characterization methods.

Schönfeld et al characterizes the mixing performance by examining the interfacial stretching within the flow using the Lyapunov exponent value. In two dimensional geometries, chaotic flows exhibit efficient mixing due to an exponential increase of interfacial stretching over time. No Lyapunov exponent values are reported; however, the literature reports efficient homogenous mixing achieved by one step of the SAR mixer with low Reynolds number, whereas the lamellae layers break down with increasing Reynolds number. For our two-dimensional investigation at Re = 1, efficient homogenous mixing was achieved in one step by the standards of the mixing cup and optical concentration values of 0.5 and mixing cup and

optical variances of 0.128 and 0.147 respectively. The target concentration value of 0.5 was maintained with the geometry in series and the two variances decreased slightly with each additional step of the five steps investigated. Therefore, mixing cup and optical concentration characteristics verify the efficient mixing of the two-dimensional SAR mixer model at low Reynolds numbers, as expected from the results of the literature.

The formation of lamellae layers was examined with the flow solver CFX 5.6 in the literature, whereas COMSOL Multiphysics 3.4 is used for our investigation. The literature examines the decreasing homogeneity in the layers with increasing Reynolds number. Our two-dimensional model examines flow over varying Peclet numbers (to examine flows with varying diffusion properties) and assumes a very low Reynolds number of 1 to investigate laminar flow. In the literature, the lamella configuration is relatively homogenous at $Re = 3.5$, and this was also visually confirmed through the concentration profile results of our model over all Peclet numbers. Higher Peclet numbers (500 to 1000) give more pronounced and defined homogenous lamellae layers; achieving completely uniform mixing requires more of the geometry in series. Lower Peclet numbers (100 to 500) mixes more quickly and the lamellae layers are less pronounced in just one step of the geometry, which leads to more efficient mixing over time compared to higher Peclet numbers. The breakdown in lamellae layers in the literature was seen with higher Reynolds numbers; in our model the lamellae layers broke down quickly in cases with low Peclet numbers or more than one geometry step.

Finally, the literature also examines the effects of the mixing with the geometry repeated in series. In particular, the lamellae layer formation stays extremely homogenous and defined in an 85% glycerol-water solution and a Reynolds number of 0.22. The literature finds homogenous lamination continues with 9 steps whereas our model, at a Reynolds number of 1 and Peclet numbers from 100 to 1000, loses any defined lamination at Peclet numbers lower than 500 or more than one step of the geometry. This could be due to the difference in physical properties used between the literature and in our model, as well as in the geometry definitions. While both Reynolds numbers are low enough that the flow rate between the two results should not be an issue, the literature model has standard dimensions of 1mm as a channel width and 6mm as a step length whereas our model has a standard channel width of 0.2 mm and a length of 1.2 mm. The difference between the examined model from the literature could be due to differences in diffusion properties, density and viscosity standards, where the literature

experiment with water-blue dye in the 85% glycerol-water solution must have a higher Peclet number than 1000, suggesting a lower diffusion constant, and also a higher fluid density due to the solution make-up.

An examination of the three-dimensional model results will leads to visual verification of the formation of homogenous lamellae layers in one step and in series. Currently, our model produces the expected layers best at high Peclet numbers, but these layers are less defined with an increased number of steps in series. The expected behavior set forth by the literature is confirmed; however, better lamination could be achieved through a manipulation of the physical properties investigated. An examination of varying Reynolds numbers for the COMSOL-generated model would also be helpful for further comparison to the literature model.

VI. Conclusions

The target mixing cup concentration of 0.5 is approached in one step of the optimal SAR mixer geometry. Uniform mixing is encouraged by elongating the geometry or by increasing the steps of the geometry in series. Lamellae layer formation is better achieved with a smaller number of steps (ideally one to two) and higher Peclet numbers. The optical concentration variance is only very slightly larger than the mixing cup concentration variance for a single step over all Peclet number ranges, suggesting no strong deviation between the two. The variances for Peclet numbers between 100 and 1000 are between the ranges of roughly 0.00 to 0.14, and the trend varies for a series of mixers depending on the Peclet number value.

The variances over constant Peclet number and increasing steps (the number of the mixer in series) stayed relatively constant, whereas a decreasing trend in the variance over increasing steps is expected due to the improved mixing with additional series. Only a slight decrease in value from 0.01 to 0.05 was seen ranging between steps 1 through 5.

The differences in concentration characteristics between the two-dimensional and three-dimensional models differ slightly enough for both the mixing cup and optical concentration and variance values. This suggests that the two-dimensional model is sufficient for modeling the optimized SAR mixer geometry. This conclusion, however, must account for the limitations in the geometry modeled even in the three-dimensional approximation. The stacked inlets and z-directional depth changes in the shape were not accounted for and may have some effect on the overall concentration characteristics.

In general, both the two-dimensional and three-dimensional models demonstrate efficient mixing on the basis of the mixing cup concentration and optical concentration values equating close to 0.5 (from an inlet step concentration profile of 1 and 0). The variances are all well below the limit of 0.25, where the maximum variance is 0.128 for the 2-dimensional model with 1 step and a Peclet number of 1000, and 0.147 for the 3-dimensional model, both with 1 step and a Peclet number of 1000. With decreasing Peclet number and an increasing number of steps, the variances decrease to values as low as 0.006 (for 5 steps at Peclet number of 100) due to the improved mixing. Therefore, the optimized SAR geometry is best when operated with a higher number of steps and lower Peclet numbers, yet still demonstrates excellent mixing with 1 step and at a Peclet number of 1000. This expectation was set forth by the literature and verified through the two-dimensional and three-dimensional modeling performed in COMSOL Multiphysics 3.4.

VI. Appendix

References

1. Finlayson, B. A. *Introduction to Chemical Engineering Computing.* John Wiley & Sons, Inc., Hoboken: 2006.

2. Koch, M. V., VandenBussche, K.M., and Chrisman, R.W., eds. *Micro Instrumentation for High Throughput Experimentation and Process Intensification – a Tool for PAT.* John Wiley & Sons, Inc., Hoboken: 2007.

3. Schönfeld, F. et al. "An optimized split-and-recombine micro-mixer with uniform 'chaotic' mixing." *Lab Chip*, 2004, **4**, 65-69.

Raw Results

Original Values (2D geometry):

		654	2616	10464
Elements		654	2616	10464
DOF		4539	17579	69615
Mesh #		**1**	**2**	**3**
$\int c$		0.506	0.504	0.500
$\int v$		2.000	1.995	1.998
$\int c*v$		1.010	1.006	0.999
c_{mix}		0.505	0.504	0.500
$\int(c-c_{mix})^2*v$		0.119	0.252	0.256
$c_{var} \int(c-c_{mix})^2$ **(no v)**		0.119	0.148	0.147
c_{var} **v**		0.060	0.126	0.128
_P (N/m)		85.924	85.471	85.387
Dimensional _P		0.430	0.427	0.427

Original Values (3D geometry):

Points		661	2092	6341
Elements		2360	9270	30081
DOF		34900	76495	201852
Mesh #		**1**	**2**	**3**
int c		0.505	0.514	0.507
int v		1.522	1.522	1.522
int c*v		0.795	0.774	0.750
cmix		0.522	0.509	0.493
var int(c-cmix)2*v		0.121	0.162	0.192
var int(c-cmix)2 no v		0.167	0.141	0.147

cvar v	0.080	0.106	0.126
delta P (N/m)	176.131	176.131	176.131
nondim delta P	0.881	0.881	0.881

For mixers in series:

c_{var} mixing cup over increasing Peclet Number -->

# Mixers in Series	100	200	300	500	750	1000
1	0.008	0.026	0.046	0.086	0.114	0.128
2	0.002	0.007	0.016	0.045	0.075	0.097
3	0.001	0.003	0.006	0.020	0.043	0.064
4	0.000	0.002	0.003	0.007	0.017	0.028
5	0.000	0.001	0.002	0.006	0.013	0.021

c_{var} optical over increasing Peclet Number -->

# Mixers in Series	100	200	300	500	750	1000
1	0.006	0.034	0.063	0.103	0.132	0.148
2	0.002	0.012	0.028	0.057	0.091	0.116
3	0.001	0.005	0.012	0.031	0.054	0.079
4	0.001	0.001	0.006	0.016	0.029	0.035
5	0.000	0.002	0.004	0.010	0.023	0.032

c_{var} optical over increasing Peclet Number -->

# Mixers in Series	100	200	300	500	750	1000
1	0.006	0.034	0.063	0.103	0.132	0.148

LN(cvar) optical over increasing Peclet Number -->

# Mixers in Series	100	200	300	500	750	1000
1	-5.191	-3.385	-2.766	-2.270	-2.028	-1.907

Sample Calculations

For a single step, mesh #1, the mixing cup concentration is given as:

For a single step, mesh #1, the mixing cup concentration variance is given as:

For a single step, mesh #1, the optical concentration is given as:

For a single step, mesh #1, the optical concentration variance is given as:

For a single step, mesh #1, the dimensionless press drop is: